Hindawi
Geofluids
Volume 2019, Article ID 8268050, 14 pages
https://doi.org/10.1155/2019/8268050

Research Article

Adsorption Equilibrium and Thermodynamic Analysis of CO_2 and CH_4 on Qinshui Basin Anthracite

Xidong Du,[1,2] Tengfei Wu,[1,3,4] Fulong Sun,[3,4] Zhenkun Hou,[5] Zhenjian Liu,[6] Liang Huo,[1,2] Yu Hao,[7] and Yuan Zhao[8]

[1]*Key Laboratory for Digital Land and Resources of Jiangxi Province, East China University of Technology, Nanchang 330013, China*
[2]*School of Earth Sciences, East China University of Technology, Nanchang 330013, China*
[3]*China Coal Technology and Engineering Group Shenyang Research Institute, Fushun 113122, China*
[4]*State Key Laboratory of Coal Mine Safety Technology, Fushun 113122, China*
[5]*Guangzhou Institute of Building Science Co., Ltd., Guangzhou 510440, China*
[6]*College of Civil Engineering, Yancheng Institute of Technology, Yancheng, Jiangsu 224051, China*
[7]*College of Mining and Environmental Engineering, Chongqing Vocational Institute of Engineering, Chongqing 402260, China*
[8]*Sinohydro Bureau 8 Co. Ltd., POWERCHINA, Changsha 410004, China*

Correspondence should be addressed to Tengfei Wu; tfwu1990@126.com and Yuan Zhao; zhao.yuan@cqu.edu.cn

Received 28 June 2019; Revised 19 November 2019; Accepted 29 November 2019; Published 21 December 2019

Academic Editor: Umberta Tinivella

Adsorption isotherms of CH_4 and CO_2 on Qinshui Basin anthracite were obtained at the temperatures of 283 K, 303 K, and 323 K using the gravimetric method. The feasibility of the displacement of CH_4 by injecting CO_2 on this anthracite was verified by calculating the selectivity factor of CO_2 over CH_4 (α_{CO_2/CH_4}), adsorption affinities, and thermodynamic properties of CH_4 and CO_2. Results show that the values of α_{CO_2/CH_4} are more than 4.0. Henry's constant (K_H) of CH_4 is smaller than that of CO_2, and CH_4 has a weaker affinity with coal surface. As temperature improves, K_H of CO_2 and CH_4 decrease. Gibbs free energy change (ΔG) and surface potential (Ω) of CO_2 are more negative than those of CH_4, indicating that CO_2 adsorption on anthracite is more spontaneous and favorable. The absolute values of Ω and ΔG of CH_4 and CO_2 increase with pressure rises. Isosteric heat of adsorption (Q_{st}) of CH_4 is lower than that of CO_2. With increasing loading, Q_{st} and entropy loss (ΔS) of CH_4 decrease, while Q_{st} and ΔS of CO_2 increase. The higher ΔS of CO_2 reveals that the adsorbed CO_2 molecules constitute a more stable rearrangement than CH_4 molecules. High temperature reduces ΔS of CH_4 and CO_2.

1. Introduction

In the last few decades, coalbed methane has gradually grown in significance as an alternative to conventional natural gas resource due to its low pollution, abundant reserves, and wide distribution [1]. Meanwhile, coalbed methane is deemed as a dangerous gas for the underground coal mining activity, as the release of CH_4 during coal mining process can potentially result in the risk of gas explosion and coal and gas outburst [2]. The effective exploitation and disposition of coalbed methane is essential for the safe mining of coal. With the worsening of the global greenhouse effect, the sequestration of anthropogenic CO_2 into deep geological formations, such as deep unmineable coal seams, saline aquifers, depleted oil and gas reservoirs, and shale gas sediments, has received lots of attention [3–6]. Based on the higher adsorption affinity of CO_2 over CH_4 on coal surface, injected CO_2 can competitively displace the preadsorbed CH_4 out of micropores and subsequently stay in the fracture and coal matrix [4], which is a promising technology that has the benefits of enhanced coal methane recovery and CO_2 sequestration in a geological time scale.

The underlying principle of the technology of enhanced coal methane recovery by CO_2 injection (CO_2-ECBM) is

the competitive adsorption between injected CO_2 and preadsorbed CH_4. More than 80% of coalbed methane is stored in the form of adsorbed gas [7]. Investigation about the adsorption performances of CH_4 and CO_2 on coal could provide useful information to understand the adsorption mechanisms of CH_4 and CO_2 and verify the feasibility of the technology of CO_2-ECBM. To date, many studies have addressed the adsorption behaviors of CH_4 and CO_2 on different rank coals by the means of laboratory experiment and numerical simulation analysis [2, 8–17]. Their results indicate that the adsorption amount and adsorption rate of CO_2 on coal are larger than those of CH_4 [2, 13, 16]. The adsorption abilities of CH_4 and CO_2 on coal are tightly related to the reservoir condition (pressure, temperature, and effective stress) and the physical-chemical property of coal (mineral composition, total organic carbon content, ash content, pore structure, surface functional group, and moisture content) [8–12, 14, 16, 17]. Various adsorption models including the Langmuir model, Brunauer-Emmett-Teller (BET) model, and pore-filling model are capable of dealing with the adsorption data of CH_4 and CO_2 on coal [2, 14, 15, 17, 18]. The values of selectivity factor of CO_2 over CH_4, which is a key indicator to assess the displacement efficiency of CO_2, are all higher than one on different rank coals [8, 13, 15–18].

Adsorption processes are often accompanied by heat generation and changes in the entropy and enthalpy of the adsorption system. Research about the interaction between coal matrix surface and adsorbate molecule from the thermodynamic point of view is conducive to comprehending the intrinsic adsorption mechanisms of CH_4 and CO_2 on coal. The adsorption thermodynamic properties viz., isosteric heat of adsorption (Q_{st}), surface potential (Ω), Gibbs free energy change (ΔG), enthalpy change (ΔH), and entropy change (ΔS), have specific physical meaning to illustrate the adsorption phenomenon. At present, the thermodynamics of adsorption of CH_4 and CO_2 on porous materials, such as shale, carbon molecular sieves, activated carbon fiber, and zeolite 13X, have been analyzed [19–22]. Duan et al. [19] investigated the thermodynamics of CH_4 and CO_2 on Sichuan Basin marine shale. They found that the absolute values of entropy loss, Gibbs free energy change, and surface potential of CO_2 are bigger than those of CH_4, and CO_2 molecules constitute a more stable and ordered arrangement on matrix surface. Song et al. [20] conducted the thermodynamic analysis of CH_4 and CO_2 on three carbon molecular sieves. Their results indicated that with increasing surface coverage, the absolute value of entropy change rises, while the absolute value of Gibbs free energy reduces. Zhou et al. [21] discussed the thermodynamic characteristic of CO_2 on activated carbon fiber and suggested that the Gibbs free energy change of CO_2 increases smoothly over the whole pressure range, whereas the entropy loss decreases continuously. Mofarahi and Bakhtyari [22] estimated the thermodynamic parameters of CH_4 on zeolite 13X. They observed that adsorption loading has no influence on the isosteric adsorption heat of CH_4 at lower degree of coverage, and the absolute values of Gibbs free energy and surface potential increase with enhancing equilibrium pressure.

There are also some studies on the thermodynamic behaviors of CH_4 and CO_2 on coal [13, 14, 23, 24]. Busch and Gensterblum [14] revealed that the isosteric adsorption heats of CH_4 and CO_2 on coal both gradually reduce with the increase of moisture content. Zhou et al. [23] discovered that the change of Gibbs free energy after CO_2 adsorption on coal is higher than that after CH_4 adsorption, and the initial isosteric adsorption heats of CO_2 and CH_4 are 48.2 and 33.4 kJ/mol, respectively. Dong et al. [24] performed a molecular simulation study about the adsorption of CH_4 and CO_2 on middle-rank coal, and reported that with the increase of sorption loading, Q_{st} of CO_2 and CH_4 reduce at first, and then slowly rise. In addition, Q_{st} of CH_4 is lower than that of CO_2 at the same adsorbed density. You et al. [13] researched the adsorption behaviors of CH_4, CO_2, and their mixtures on bituminous coal by the means of numerical simulation. Their results showed that Q_{st} of CH_4 and CO_2 both decrease with increasing adsorption amount, and this decline is due to the presence of heteroatom functional groups. Apparently, the thermodynamic characteristics of CH_4 and CO_2 on coal, especially the surface potential and entropy change, require further study. Therefore, it is of fundamental importance to perform the detailed thermodynamic analysis of CO_2 and CH_4 on coal.

In this paper, the adsorption isotherms of CH_4 and CO_2 on anthracite were measured using the accurate gravimetric method at the temperatures of 283 K, 303 K, and 323 K and pressures up to 1.80 MPa. The Langmuir-Freundlich model was adopted to fit the adsorption data. The selectivity factor of CO_2 over CH_4 on anthracite was predicted based on the single component adsorption isotherm using ideal adsorbed solution theory. Henry's constant was estimated and used to analyze the affinity between adsorbate and coal matrix surface. Adsorption thermodynamic parameters of CH_4 and CO_2 on coal were calculated and discussed. This research will lay the foundation for the better understanding of the adsorption mechanisms of CH_4 and CO_2 on coal and provide guide for the future application of the technology of CO_2-ECBM.

2. Material and Method

2.1. Material Preparation and Characterization

2.1.1. Material Preparation. The Qinshui (QS) anthracite adopted in this study was sampled from the southern district of Qinshui Basin of China at the depth of 350 m. Before measurement and characterization, the bulk coal was crushed and sieved into 0.85 to 0.425 mm particles.

2.1.2. Characterization of Coal Sample

(1) Mesopore and Macropore Morphology Analysis. The mesopore and macropore structures of this anthracite were analyzed with an ASAP 2020M system (Micromeritics Instruments, USA), using a low-pressure N_2 adsorption at 77 K. The BET surface area (S_{BET}), macropore volume (V_{mac}), mesopore volume (V_{mes}), micropore volume (V_{mic}), total volume (V_t), and pore size distribution (PSD) were obtained based on N_2 adsorption isotherm data.

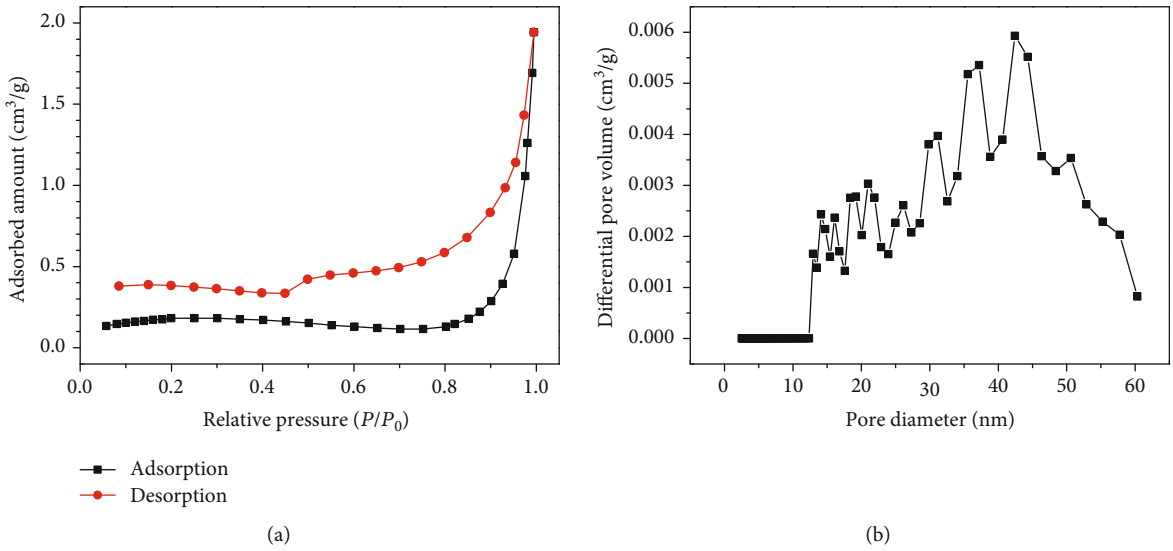

Figure 1: N_2 adsorption and desorption isotherms at 77 K (a) and the pore size distribution of mesopore and macropore (b).

Table 1: Pore structure parameters of QS sample determined from N_2 and CO_2 adsorption.

	N_2 adsorption				CO_2 adsorption	
S_{BET} (m^2/g)	V_{mic} (cm^3/g)	V_{mes} (cm^3/g)	V_{mac} (cm^3/g)	V_t (cm^3/g)	S_{DR} (m^2/g)	V_{DR} (cm^3/g)
0.62	0	0.0018	0.0005	0.0023	58.59	0.023

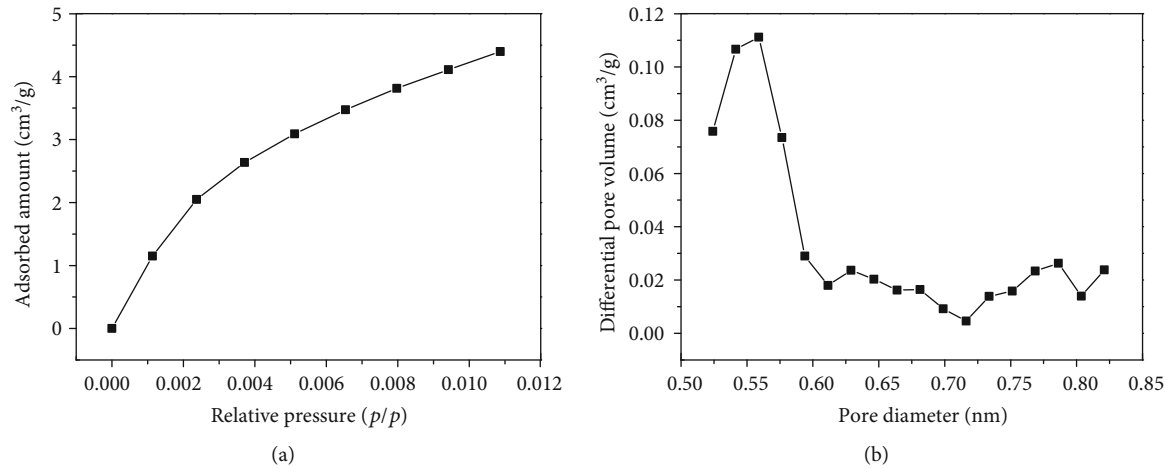

Figure 2: CO_2 adsorption isotherm at 273.15 K (a) and micropore size distribution (b).

The desorption and adsorption isotherm data of N_2 at 77 K are shown in Figure 1(a). The PSD of QS sample determined by N_2 adsorption is depicted in Figure 1(b). The estimated mesopore and macropore parameters are listed in Table 1.

The hysteresis loop between adsorption and desorption curves belongs to type H2 based on the definition of International Union of Pure and Applied Chemistry (IUPAC). The type of this hysteresis loop indicates that the pore of QS anthracite is slit shape. The PSD shown in Figure 1(b) indicates that QS anthracite has continuous wide meso/macropore size distribution from 13 nm to 60 nm. In addition, it can be found from Table 1 that QS anthracite has a lot of mesopores (pore size of 2-50 nm) whose volume (V_{mes}) is much larger than the volume of macropore (V_{mac} of pore size larger than 50 nm).

(2) Micropore Morphology Analysis. The micropore structure of QS sample was also obtained using ASAP 2020M system by CO_2 adsorption at 273.15 K. The micropore surface area (S_{DR}) and micropore volume (V_{DR}) were calculated by the Dubinin-Radushkevich (DR) model based on CO_2 adsorption data. The micropore size distribution was determined by the nonlocal density functional theory (NLDFT) model.

The adsorption isotherm of CO_2 at 273.15 K is shown in Figure 2(a). The estimated micropore parameters are listed in Table 1. The micropore size distribution of QS sample

Table 2: Results of ultimate and proximate analyses of QS anthracite.

Sample	Coal rank	Ultimate analysis (wt% daf)				Proximate analysis (wt%)			
		C	H	N	O	C_{fix}	V_{daf}	A_{ad}	M_{ad}
QS	Anthracite	90.01	3.75	0.94	2.01	70.73	10.42	18.55	3.62

Note: C_{fix}: fixed carbon; V_{daf}: volatile matters; A_{ad}: ash; M_{ad}: moisture.

determined by CO_2 adsorption is depicted in Figure 2(b). We can find that QS anthracite has a broad micropore distribution with major peak at around 0.55 nm.

It is noticeable that the value of S_{DR} of 58.59 m^2/g is much higher than that of S_{BET} of 0.62 m^2/g. Meanwhile, the value of V_{DR} of 0.023 cm^3/g is bigger than those of V_{mes} of 0.0018 cm^3/g and V_{mac} of 0.0005 cm3/g. Therefore, the surface and pore volume of QS anthracite are mainly contributed by micropore, and micropore will provide a large number of adsorption sites for the adsorption of CH_4 and CO_2 on this anthracite.

(3) Ultimate and Proximate Analyses. Ultimate and proximate analyses were used to characterize coal chemical composition. Ultimate analysis was performed by Flash EA2000 elemental analyzer, Thermo Fisher Scientific. The results of ultimate and proximate analyses of this anthracite are given in Table 2. It is clear that carbon, hydrogen, oxygen, and nitrogen are the main elements in coal reservoir, accounting for more than 95% of the total element content.

2.2. Adsorption Isotherm Measurement and Simulation. A high-resolution intelligent gravimetric analyzer (IGA-100B, U.K.) was employed to measure the adsorption isotherms of CH_4 and CO_2 at pressure up to 1.80 MPa and at temperatures of 283 K, 303 K, and 323 K.

Adsorption isotherm can offer useful information about the surface property of porous material and the interaction between adsorbent and adsorbate [25]. Meanwhile, adsorption isotherm simulation is of great importance for the prediction of adsorption capacity and the interpretation of adsorption mechanism. In this study, the Langmuir-Freundlich (L-F) model was applied to simulate the adsorption data of CH_4 and CO_2. The L-F model is described in the following form [26]:

$$q = \frac{q_m b P^c}{1 + bP^c}, \tag{1}$$

where q is the adsorption amount at pressure P; q_m is the saturation adsorption capacity of adsorption sites; b is the affinity coefficient of adsorption sites; and c is equal to $1/n$, where n is the deviation from an ideal homogenous surface.

2.3. Ideal Adsorbed Solution Theory. The adsorption of binary gas mixtures can be directly predicted from pure component adsorption data using ideal adsorbed solution theory (IAST) proposed by Myers and Prausnitz [27]. Many studies have confirmed the effectiveness of IAST to predict the adsorption of mixture gases on a variety of porous materials [28–30].

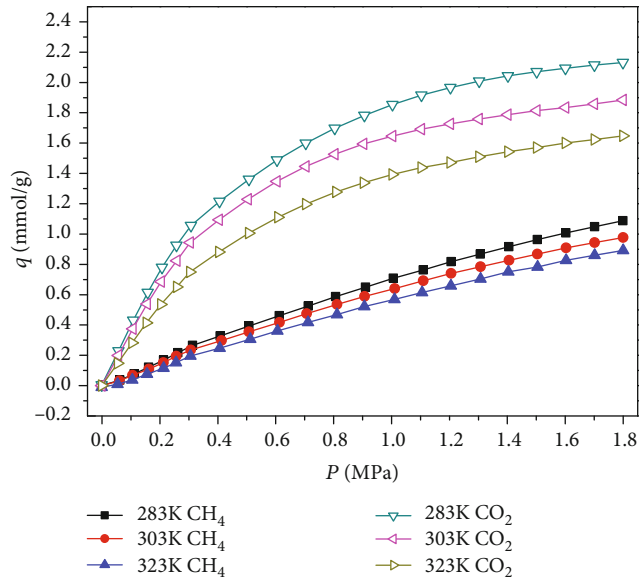

Figure 3: Adsorption isotherms of CO_2 and CH_4 at different temperatures on anthracite.

When the adsorption equilibrium of mixture gases is reached, the chemical potential of each component in the adsorbed phase is equal to that of the corresponding component in the gas phase [31]. Based on this criterion of thermodynamics equilibrium, it can be concluded that

$$P_t y_i = P_i^0(\pi) x_i, \tag{2}$$

where P_t is total pressure of adsorption system; y_i and x_i are the mole fractions of pure component i in the bulk gas phase and the adsorbed phase, respectively; P_i^0 is the equilibrium gas phase pressure of component i at the mixture temperature and spreading pressure (π).

For the binary mixture gases, the following equations are satisfied [32]:

$$\begin{aligned} P_t y_1 &= P_1^0 x_1, \\ P_t(1 - y_1) &= P_2^0(1 - x_1), \end{aligned} \tag{3}$$

where y_1 and x_1 are the mole fractions of component 1 in the bulk phase and adsorbed phase, respectively; P_1^0 and P_2^0 are the equilibrium gas phase pressures of component 1 and component 2 at the mixture temperature and spreading pressure, respectively.

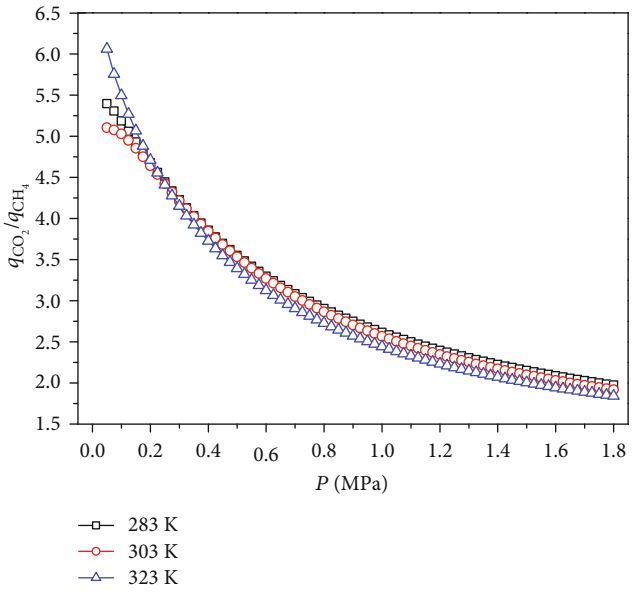

Figure 4: Ratios of adsorption amount of CO_2 relative to CH_4 at different temperatures.

The spreading pressure π and the reduced spreading pressure π^* are defined by [31]:

$$\pi = \frac{RT}{A}\int_0^{P_i^0}\frac{q}{P}dP, \tag{4}$$

$$\pi^* = \frac{A\pi}{RT} = \int_0^{P_i^0}\frac{q}{P}dP, \tag{5}$$

where T is the temperature, R is the universal gas constant, and A is the surface area of adsorbent per unit mass.

Substituting Equation (1) into Equation (5), it can be found that

$$\pi^* = \frac{1}{c}q_m \ln\left(1 + b\left(P_i^0\right)^c\right). \tag{6}$$

When the adsorption of binary mixture gases reaches equilibrium, the reduced spreading pressures of component 1 and component 2 are equal.

$$\begin{aligned}\pi_1^* &= \pi_2^*,\\ \pi_1^* &= \frac{1}{c_1}q_{m1}\ln\left(1 + b_1\left(P_1^0\right)^{c_1}\right),\\ \pi_2^* &= \frac{1}{c_2}q_{m2}\ln\left(1 + b_2\left(P_2^0\right)^{c_2}\right),\end{aligned} \tag{7}$$

where π_1^* and π_2^* are the reduced spreading pressures of component 1 and component 2, respectively; c_1 and c_2 are the L-F coefficients of component 1 and component 2, respectively; q_{m1} and q_{m2} are the saturation adsorption capacities of component 1 and component 2, respectively; b_1 and b_2 are the affinity coefficients of component 1 and component 2, respectively.

Table 3: Physical and chemical characteristics of CO_2 and CH_4 molecules.

Adsorbate	CO_2	CH_4
Kinetic diameter (nm)	0.33	0.38
Shape	Linear	Tetrahedron
Quadrupole moment (10^{-26} esu·cm^2)	4.30	0
Dipole moment (10^{-26} esu·cm^2)	0	0
Polarizability (10^{-25} cm^3)	29.1	25.9
Boiling point (K)	216.55	111.65

Combing Equations (3–7) and (8) leads to:

$$\begin{aligned}&\frac{1}{c_1}q_{m1}\ln\left(1 + b_1\left(\frac{P_t y_1}{x_1}\right)^{c_1}\right)\\ &\quad - \frac{1}{c_2}q_{m2}\ln\left(1 + b_2\left(\frac{P_t(1-y_1)}{1-x_1}\right)^{c_2}\right) = 0.\end{aligned} \tag{8}$$

For the given P_t and y_1, the value of x_1 can be obtained by Equation (8).

The selectivity factor α can be decided by:

$$\alpha = \frac{x_1/y_1}{x_2/y_2}, \tag{9}$$

where y_2 and x_2 are the mole fractions of component 2 in the bulk gas phase and adsorbed phase, respectively.

2.4. Henry's Law Constant. Henry's constant (K_H) can be applied to calculate the affinity between adsorbent surface and adsorbate molecule. Molecule-surface forces predominate at low pressure, and Henry's constant is directly related to the interaction of matrix surface with adsorbate molecule [33]. A larger K_H reflects the stronger affinity between adsorption pair.

In order to calculate K_H, the relationship between adsorption amount and equilibrium pressure can be expressed by a virial equation [34]:

$$\ln\left(\frac{q}{P}\right) = A_0 + A_1 q + A_2 q^2 + \cdots, \tag{10}$$

where A_0, A_1, and A_2 are the virial coefficients. The first virial coefficient A_0 is related to Henry's constant, as $K_H = \exp(A_0)$. At the low-pressure range, q is small, and the high-order terms in Equation (10) can be neglected. Thus, Equation (10) can be written as follows:

$$\ln\left(\frac{P}{q}\right) = -A_0 - A_1 q. \tag{11}$$

By fitting the linear region of $\ln(P/q)$ vs. the loading q, A_0 and K_H can be obtained.

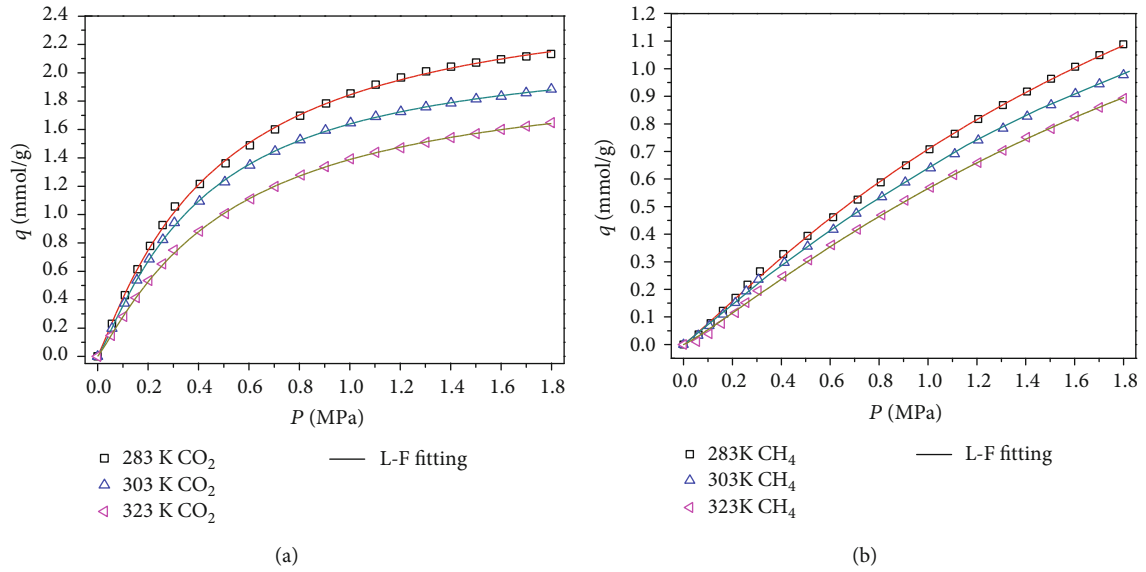

Figure 5: Simulated results of the adsorption isotherms using the L-F model: (a) CO_2 and (b) CH_4.

Table 4: Fitting parameters of the L-F model of the isotherms of CO_2 and CH_4.

Gas	T (K)	q_m (mmol/g)	b (MPa^{-1})	c	n	R^2_{nrc}
CO_2	283	2.629	2.346	1.102	0.907	0.9995
	303	2.354	2.250	1.065	0.939	0.9998
	323	2.044	2.116	1.124	0.890	0.9998
CH_4	283	2.671	0.361	1.089	0.918	0.9996
	303	2.498	0.343	1.072	0.933	0.9997
	323	2.318	0.323	1.136	0.880	0.9994

Note: R^2_{nrc}: the nonlinear regression coefficient.

2.5. Thermodynamics of Adsorption. The thermodynamic parameters in this paper are calculated using the following equations [19, 22, 35, 36]:

$$
\begin{aligned}
Q_{st} &= RT^2\left(\frac{\partial \ln P}{\partial T}\right)_q,\\
\ln P &= -\frac{Q_{st}}{RT} + C,\\
\Omega &= -RT\int_0^P q d(\ln P),\\
\Delta G &= \frac{\Omega}{q} = -\frac{RT\int_0^P q d(\ln P)}{q},\\
\Delta H &= -Q_{st},\\
\Delta S &= \frac{\Delta H - \Delta G}{T},
\end{aligned}
\tag{12}
$$

where C is the integration constant.

3. Results and Discussion

3.1. Adsorption Isotherms of CO_2 and CH_4 on Anthracite. The adsorption isotherms of CO_2 and CH_4 at three temperatures are shown in Figure 3. We can find that the adsorption amounts of CO_2 and CH_4 increase monotonically with increasing equilibrium pressure. For the adsorption of CO_2 on coal, the adsorption rate is faster at low-pressure range. As pressure enhances, CO_2 adsorption rate gradually decreases. For the adsorption of CH_4 on coal, the adsorption rate is almost the same over the whole pressure range. The adsorption amounts of both gases at three temperatures are as follows: 283 K > 303 K > 323 K. High temperature will be detrimental to gas adsorption on anthracite, especially for the adsorption of CO_2. This is mainly because increasing temperature will give the adsorbate molecules more energy to overcome the van der Waals force and electrostatic interaction and stay in the gas phase [21]. On the shale organic nanochannels, the effect of temperature on CH_4 adsorption is more remarkable [37]. Meanwhile, the adsorption isotherms of both gases belong to type I according to the IUPAC classification, which indicates that the adsorbent sample is typically microporous material conforming to the result of the characterization of pore structure of this anthracite.

At the same condition, the adsorption quantity of CO_2 on anthracite is much higher than that of CH_4. The ratios of adsorption amount of CO_2 relative to CH_4 (q_{CO_2}/q_{CH_4}) at three temperatures are displayed in Figure 4. We can find that the values of q_{CO_2}/q_{CH_4} range from 1.8 to 6.1, and these values are in coincidence with previous reports [1, 9, 10, 12, 38]. More than 1.8 of the value of q_{CO_2}/q_{CH_4} verifies the possibility of the displacement of adsorbed CH_4 by injecting CO_2. With elevating equilibrium pressure, q_{CO_2}/q_{CH_4} declines. It seems that the continuous decrease of the adsorption rate of CO_2 and the minor change of the adsorption rate of CH_4 can account for the downward trend of q_{CO_2}/q_{CH_4}. At

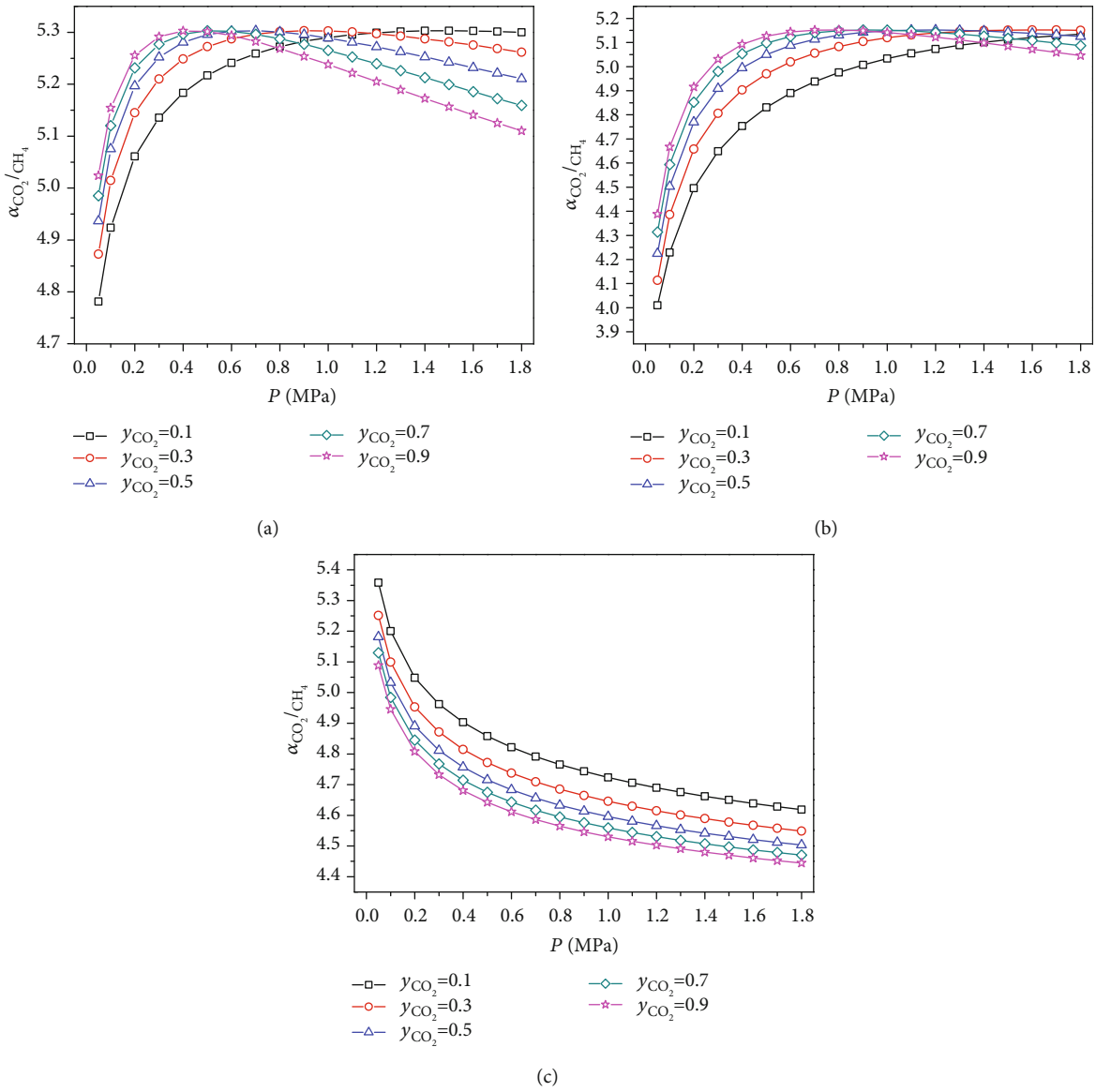

Figure 6: Predicted adsorption selectivity of CO_2 over CH_4 at different temperatures: (a) 283 K, (b) 303 K, and (c) 323 K.

pressure lower than 0.2 MPa, q_{CO_2}/q_{CH_4} is the biggest at 323 K, while at 303 K q_{CO_2}/q_{CH_4} is the smallest. When the pressure is higher than 0.2 MPa, low temperature is beneficial to obtaining bigger q_{CO_2}/q_{CH_4}.

The larger adsorption capacity of CO_2 than CH_4 on coal is attributed to the different characteristics of CH_4 and CO_2. Table 3 summarizes the physical and chemical properties of CO_2 and CH_4 molecules. The smaller kinetic diameter and the linear shape of CO_2 molecule allow CO_2 to diffuse into the more restricted inner pore spaces where the entry of CH_4 is not permitted. Relevant research has shown that CO_2 molecule can diffuse into an additional 40% of the organic pore structure compared with CH_4 molecule [39]. Besides, CH_4 is nonpolar, while CO_2 has a permanent quadrupole moment. This quadrupole moment can lead to the intensive electrostatic interaction between CO_2 molecule and porous adsorbent surface [20] and thereby the larger adsorption quantity. Meanwhile, the boiling point of CH_4 is lower than that of CO_2. The fluid with higher boiling point is easily adsorbed to porous material, as the fluid with higher boiling point has the larger intermolecular attraction and is liable to liquefaction [40].

3.2. Simulation of Adsorption Isotherms of CO_2 and CH_4. The simulated results of the adsorption curves of CH_4 and CO_2 using the L-F model are presented in Figures 5(a) and 5(b), respectively. It is obvious that the simulated results agree well with the experimental results, revealing that the adopted L-F model is able to describe the adsorption curves of CH_4 and CO_2 on anthracite.

Table 4 lists the parameters of CH_4 and CO_2 in the L-F model. As given in Table 4, q_m for CO_2 and CH_4 both decrease with increasing temperature, implying that low temperature helps to achieve higher coalbed methane content

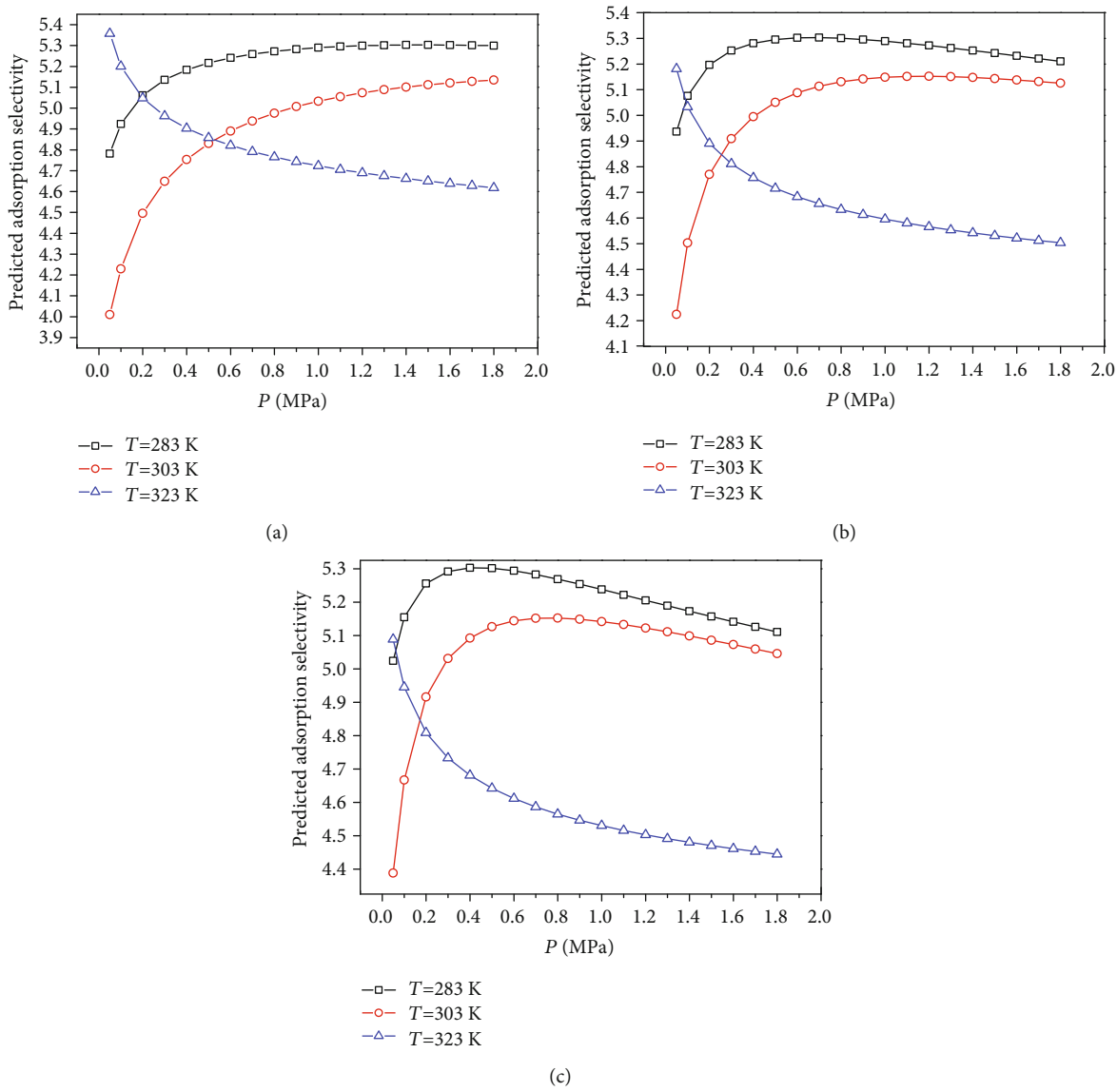

Figure 7: Comparison of predicted adsorption selectivity of CO_2 over CH_4 at three temperatures for the adsorption of different CO_2/CH_4 mixture gases: (a) $y_{CO_2} = 0.1$, (b) $y_{CO_2} = 0.5$, and (c) $y_{CO_2} = 0.9$.

Table 5: Comparison of α_{CO_2/CH_4} on different coals and shales.

Coal	Pressure P (MPa)	Temperature T (K)	α_{CO_2/CH_4}	Reference
Anthracite	0-1.80	283-323	4.00-5.30	This study
Lignite	0-1.80	288-328	4.84-5.27	Liu [18]
Bituminous	0-1.80	288-328	4.43-4.95	Liu [18]
Anthracite	0-1.80	288-328	5.03-7.97	Liu [18]
Bituminous coal model	3.04-32.25	295.70-370.20	2.00-9.00	Zhang et al. [8]
Coal molecular model	3.04-14.82	295.70-325.70	1.25-5.00	Brochard et al. [42]
Bituminous coal model	0-15	300-340	3.20-6.80	You et al. [13]
Coal surface model	0-10	298	2.20-14.50	Liu et al. [15]
Sichuan Basin shale	0-2	278-318	2.72-7.87	Duan [43]
Barnett shale	0-27.50	313	2.42	Duan [43]
Marcellus shale	0-27.50	313	4.76	Duan [43]

Table 6: Results of Henry's constant for CO_2 and CH_4 at different temperatures on anthracite.

Gases	283 K	303 K	323 K
CH_4	0.66	0.60	0.35
CO_2	4.45	3.87	2.92

and sequestrate large amounts of CO_2. Meanwhile, the values of b of both gases also decrease with the improvement of temperature. In addition, the values of n for the adsorption of CH_4 and CO_2 all deviate from the unity, which reveals that the anthracite is heterogeneous sedimentary rock. For the naturally occurring carbonaceous organic-rich materials, such as coal and shale, the most prominent feature of these solid surfaces is its inhomogeneity [41]. On the one hand, the inhomogeneity comes from lattice defects, vacancies, and dislocations in crystals. On the other hand, the presence of chemical impurities can also cause the inhomogeneity of solid surface.

3.3. Adsorption Selectivity of CO_2 over CH_4 on Anthracite. The predicted adsorption selectivity factors of CO_2 over CH_4 (α_{CO_2/CH_4}) on anthracite are illustrated in Figure 6. For an equimolar CO_2/CH_4 mixture system, $\alpha_{CO_2/CH_4} > 1$ infers that CO_2 is preferentially adsorbed in the binary mixture [37]. High selectivity implies the enrichment in the adsorbed phase of CO_2 over CH_4 compared with the ratio in gas phase [8]. It is noticeable that mole fraction of CO_2 (y_{CO_2}) in mixture gases has significant influence on α_{CO_2/CH_4}. Meanwhile, the variation trends of α_{CO_2/CH_4} at three temperatures are different.

At 283 K, with the increase of pressure, α_{CO_2/CH_4} quickly increases to the maximum and then slowly declines. In the low-pressure range, α_{CO_2/CH_4} improves with the increase of CO_2 mole fraction in mixture gases. In the high-pressure range, α_{CO_2/CH_4} decreases with increasing CO_2 mole fraction in mixture gases. At 303 K, the change pattern of α_{CO_2/CH_4} is similar to that of α_{CO_2/CH_4} at 283 K. The difference is that the inflection point of variation curve of α_{CO_2/CH_4} is delayed at 303 K. It should be noted that at 323 K, the change pattern of α_{CO_2/CH_4} is different from those of α_{CO_2/CH_4} at 283 K and 303 K. At 323 K, α_{CO_2/CH_4} continuously reduces as pressure increases. Meanwhile, the lower CO_2 mole fraction in mixture gases is helpful to obtain bigger α_{CO_2/CH_4} at 323 K. Zhang et al. [8] and You et al. [13] also observed that the adsorption selectivity of CO_2 over CH_4 declines gradually with the increase of the bulk CO_2 mole fraction.

The comparison of α_{CO_2/CH_4} at different temperatures for the adsorption of different CO_2/CH_4 mixture gases ($y_{CO_2} = 0.1$, $y_{CO_2} = 0.5$, and $y_{CO_2} = 0.9$) are depicted in Figure 7. It can be found that α_{CO_2/CH_4} at 283 K is higher than that at 303 K for the adsorption of three selected CO_2/CH_4 mixture gases. When equilibrium pressure is bigger than 0.20 MPa, α_{CO_2/CH_4} at 283 K is the highest for the adsorption of mixture gases of $10:90/CO_2:CH_4$. For the adsorption of mixture gases of $50:50/CO_2:CH_4$, α_{CO_2/CH_4} at 283 K is the highest when equilibrium pressure is bigger than 0.10 MPa. For the adsorption of mixture gases of $90:10/CO_2:CH_4$, α_{CO_2/CH_4} at 283 K is the highest when equilibrium pressure is bigger than 0.05 MPa. Generally, the technology of CO_2-ECBM is applied in deep unmineable coal seams with reservoir pressure higher than 0.5 MPa. Therefore, low temperature is beneficial for injected CO_2 to displace preadsorbed CH_4.

As shown in Figure 7, the values of α_{CO_2/CH_4} are more than 4.0, revealing that the adsorbed CH_4 on coal surface can be directly displaced by injected CO_2. The higher the α_{CO_2/CH_4} is, the higher the displacement efficiency of CO_2 is. Hence, the further application of the technology of CO_2-ECBM in this anthracite seam is feasible.

Comparison of α_{CO_2/CH_4} on different coals and shales is listed in Table 5. It is clear that the values of α_{CO_2/CH_4} in studied anthracite are within the range of the values of α_{CO_2/CH_4} in other coals reported by previous researchers [8, 13, 15, 18, 42]. This confirms that using the IAST model to calculate the values of α_{CO_2/CH_4} is reliable. In addition, the values of α_{CO_2/CH_4} on coals are comparable to those of α_{CO_2/CH_4} on shales, which shows that the technology of enhanced shale gas recovery by CO_2 injection is also feasible.

3.4. Henry's Law Constants of CO_2 and CH_4 on Anthracite. The calculated results of Henry's constant for CH_4 and CO_2 on anthracite are given in Table 6. K_H for CO_2 and CH_4 both decrease with increasing experiment temperature. High temperature can reduce the adsorption affinity of two gases on anthracite surface. Accordingly, the adsorption capacity decreases with temperature increases as shown in Figure 3. Under same condition, K_H of CH_4 is much smaller than that of CO_2, and CO_2 has stronger adsorption affinity with anthracite. The permanent quadrupole moment of CO_2 molecule, which causes stronger electrostatic interaction between CO_2 and adsorbent, brings about greater affinity of CO_2 on porous material surface [21]. As a result, the adsorption amount of CO_2 is much higher than that of CH_4 on anthracite.

3.5. Thermodynamic Analysis of Adsorption of CO_2 and CH_4 on Anthracite

3.5.1. Surface Potential. The minimum isothermal work, which is necessary to load the adsorbent to a given level, is defined as surface potential Ω [36]. The calculated results of surface potential for CH_4 and CO_2 as a function of pressure are illustrated in Figures 8(a) and 8(b), respectively. At all experiment temperatures, the absolute values of Ω of CO_2 and CH_4 rise monotonically with increasing system pressure. This is mainly because higher isotherm work is needed to fill more adsorbate molecules into cavity pores than at the initial stage of adsorption [19]. This phenomenon is also found for gas adsorption on other porous materials, such as zeolite 13X, shale, and chabazite zeolite [19, 22, 36]. Meanwhile, with the elevation of temperature, the decrease of Ω in the negative value takes place. Surface potential is a criterion of

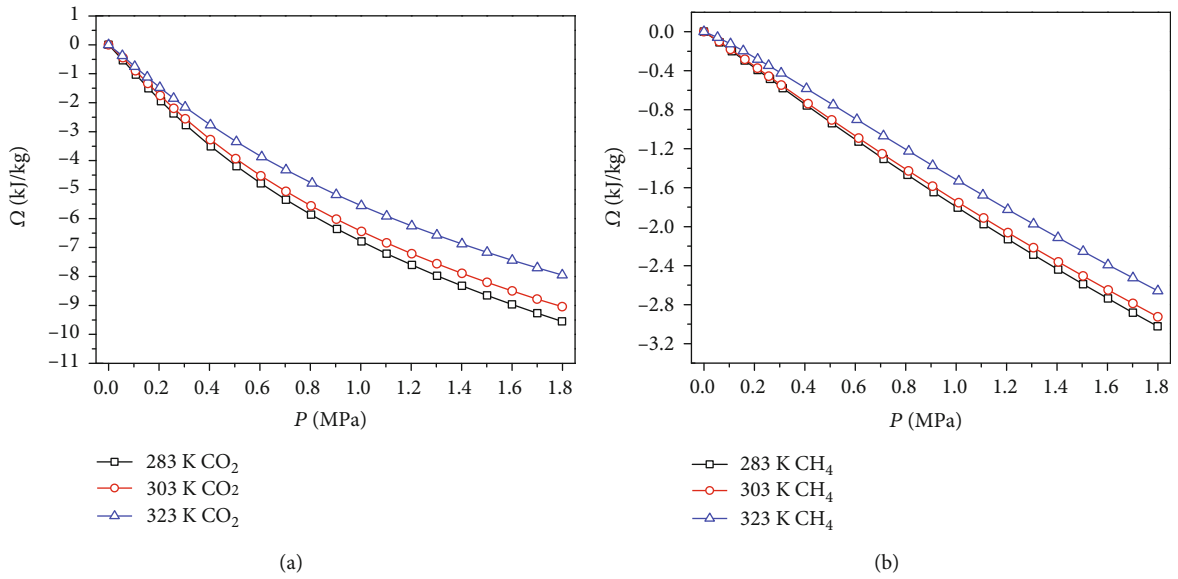

Figure 8: Surface potentials of CO_2 (a) and CH_4 (b) on anthracite at different temperatures.

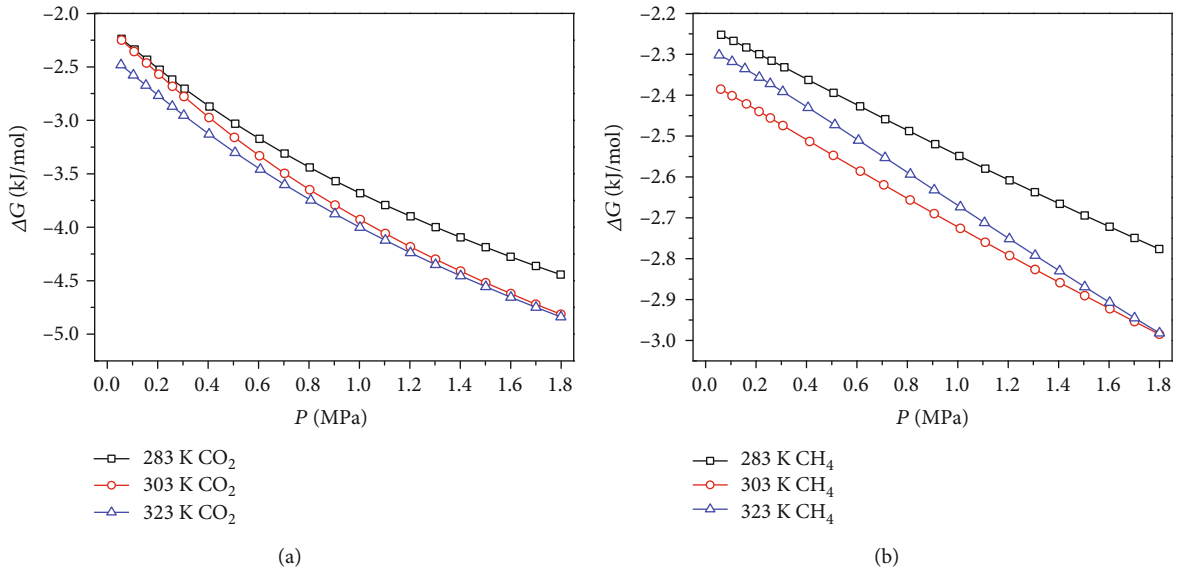

Figure 9: Gibbs free energy changes of CO_2 (a) and CH_4 (b) on anthracite at different temperatures.

necessary work to achieve the equilibrium of system. Thus, a lower equilibrium capacity leads to smaller (less negative) surface potential [33], and high temperature can reduce the absolute values of Ω of CO_2 and CH_4. It should be noted that under the same condition, the absolute value of Ω of CO_2 is much bigger than that of CH_4, revealing that CO_2 adsorption on anthracite is more favorable.

3.5.2. Gibbs Free Energy Change. Gibbs free energy refers to the increment of free energy of system with increasing adsorbent unit area at constant temperature and pressure [23]. The calculated results of Gibbs free energy change ΔG of CO_2 and CH_4 on anthracite are displayed in Figures 9(a) and 9(b), respectively. We can note that the values of ΔG of both gases are negative, implying that the adsorption processes of both gases on anthracite are spontaneous. The absolute values of ΔG of both gas rise gradually with the increase of pressure, which indicates that the degree of spontaneity of gas adsorption is larger at high pressure. Therefore, the adsorptions of CO_2 and CH_4 are more likely to occur under high pressure condition. The absolute value of ΔG of CO_2 is apparently bigger than that of ΔG of CH_4, and the degree of spontaneity of CO_2 adsorption is greater. According to the minimum energy principle, any interface has the tendency to spontaneously reduce the energy of interface. The solid interface is difficult to shrink due to the immobility of molecule or atom on interface. Thus, the surface free energy can only be reduced by adsorbing other molecule. The greater free energy change

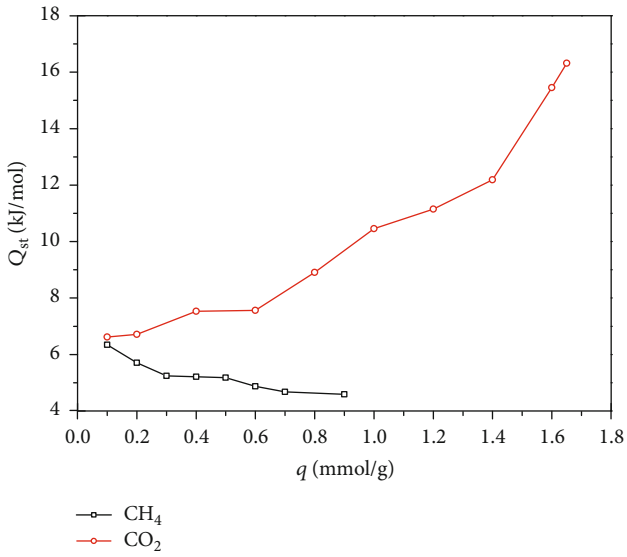

FIGURE 10: Isosteric heat of adsorption of CO_2 and CH_4 on anthracite.

results in the bigger motivation to adsorb gas and the larger adsorption quantity [23]. This is one reason why the adsorption amount of CH_4 is much smaller than that of CO_2 on anthracite.

3.5.3. Isosteric Heat of Adsorption. The heat effect of adsorption can be quantified by isosteric heat of adsorption Q_{st} ($-\Delta H$, enthalpy change). Adsorption heat can result in the change in temperature [19]. This temperature variation will cause the localized changes in the kinetic and equilibrium properties, which ultimately influences the adsorption behavior and displacement efficiency [44]. When the adsorbent surface is energetically homogeneous and the lateral adsorbate-adsorbate interaction can be neglected, Q_{st} is independent of adsorbate loading. When the adsorbent is energetically heterogeneous, Q_{st} becomes a function of adsorbate loading [45]. The degree of adsorbent heterogeneity has a strong effect on Q_{st}. The means of indirect estimation from temperature-dependent adsorption equilibrium data or direct measurement by dosing calorimetry can be adopted to acquire Q_{st} [44]. In this paper, the values of Q_{st} for CO_2 and CH_4 were obtained by the indirect estimation approach based on the adsorption isotherm data at three temperatures.

The calculated results of Q_{st} for CO_2 and CH_4 are plotted in Figure 10. The values of ΔH ($-Q_{st}$) for both gas are negative, indicating that the adsorption processes of CO_2 and CH_4 on anthracite are exothermic. Therefore, low temperature can enhance the adsorption amounts of CO_2 and CH_4. In addition, Q_{st} for CO_2 and CH_4 are not constant with the increase of adsorption amount, confirming that the studied anthracite is inherently heterogeneous. As the adsorption quantity enhances, Q_{st} of CO_2 increases consistently, whereas Q_{st} of CH_4 declines monotonously.

At the initial stage of adsorption, the available sorption sites are abundant and the lateral adsorbate-adsorbate interaction energy is lower. As adsorption loading increases, more and more cavities are occupied by adsorbate. Thus, the decrease in Q_{st} with adsorption loading takes place [46]. For the adsorption of CH_4 on anthracite, the continuous reduction of Q_{st} suggests that the interaction energy among CH_4 molecules is much weaker at higher surface coverage. With the increase of pressure (i.e., loading), more CH_4 molecules are in a free state within the pore structure of anthracite. For the adsorption of CH_4 on shale, the isosteric heat of adsorption also reduces with adsorption loading increases [19].

For CO_2 adsorption on anthracite, the intermolecular force among CO_2 molecules is gradually strengthened in the cavity pores with enhancing pressure. Compared with CH_4 molecule, CO_2 molecule with higher boiling point has the larger intermolecular attraction and is liable to liquefaction. At higher surface coverage, the stronger lateral interaction between CO_2 molecules results in the increase of Q_{st}. Similar changing trend of Q_{st} was reported by Zhou et al. for CO_2 adsorption on coal matrix [23].

Meanwhile, the value of Q_{st} of CH_4 is lower than that of CO_2. He et al. [47] have found that the hindering effect of spherical molecules caused by pore wall is smaller than that of nonspherical molecules for the same size. Contrary to regular tetrahedral CH_4 molecule, the diffusion of claviform CO_2 molecule into micropores is more influenced by inner pore walls, thereby releasing more energy and heat. During the displacement coalbed methane process, the release of heat from CO_2 adsorption will improve the temperature of coal reservoir. The rising temperature is beneficial to CH_4 desorption and the enhancement of coalbed methane recovery. Nevertheless, the increase of temperature is harmful for the sequestration of injected CO_2.

3.5.4. Entropy Change. Entropy is the measurement of disorder or patterns in which the thermodynamic system is rearranged [22]. The entropy change ΔS is a net of balance between rotation, vibration, and translation freedoms of adsorbate molecule within matrix [33]. Research about the behavior of entropy change as a function of adsorption loading helps to understand the packing manner of adsorbed molecules. The calculated results of ΔS of CO_2 and CH_4 on anthracite are shown in Figures 11(a) and 11(b), respectively. It can be seen that the values of ΔS of CO_2 and CH_4 are negative, which elucidates that the adsorption of CO_2 and CH_4 on coal surface are from a random phase to an order phase. The adsorption progress involves the reduction in the degree of freedom and the formation of a more stable rearrangement in adsorbent surface.

Relevant literature has observed that for the adsorption of CH_4 molecule, the entropy loss is between -82 and -87 J/mol/K at temperature ranging from 273 to 423 K [48]. For CH_4 adsorption on this anthracite, the value of ΔS is from -4.96 to -14.51 J/mol/K over the temperature range of 283-323 K, which is very bigger than -82 J/mol/K. The smaller entropy loss of CH_4 on anthracite implies that injected CH_4 is not completely adsorbed on coal matrix but free gas stayed in the inner pores. As illustrated in

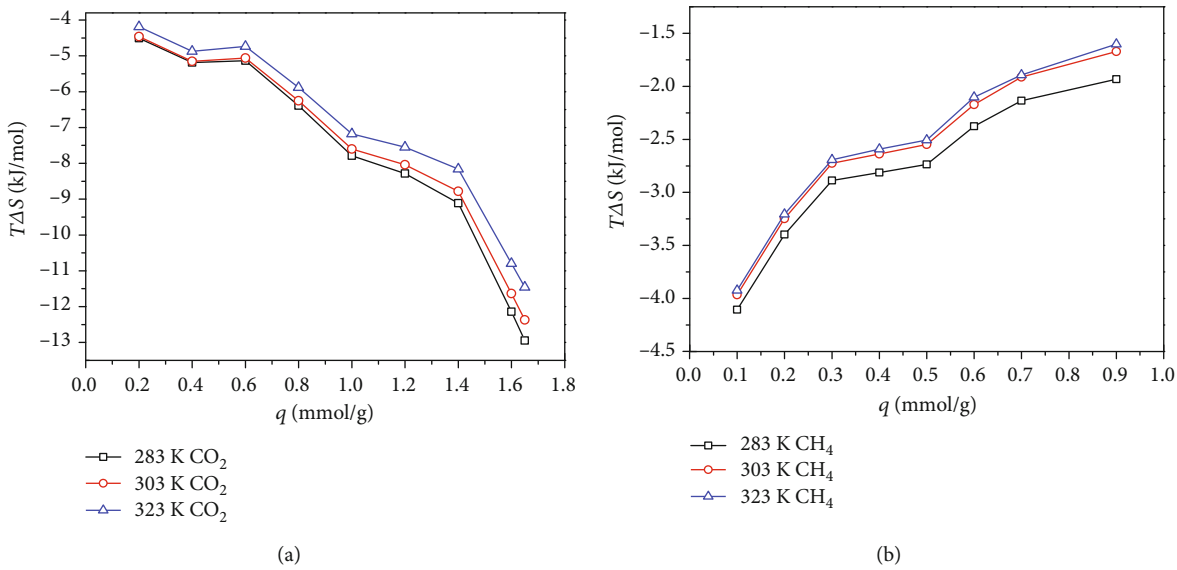

Figure 11: Entropy changes of CO_2 (a) and CH_4 (b) on anthracite at different temperatures.

Figure 11(b), the entropy loss of CH_4 reduces as adsorption amount increases. Therefore, more injected CH_4 molecules are trapped in the coal pore volume rather than adsorbed on matrix surface with increasing surface coverage, and the degree of orderliness the system becomes lower.

As illustrated in Figure 11(a), for CO_2 adsorption on anthracite, the entropy loss enhances with increasing surface coverage, inferring that the orderliness degree of the whole system becomes bigger. The increase in entropy loss is mainly because the free space in the cavity reduces, and the freedom of the adsorbate molecule becomes severely limited [21]. Hence, the adsorbed CO_2 is in a more stable state at higher surface coverage. The value of ΔS of CO_2 is from -12.97 to -45.76 J/mol/K at temperature ranging from 283 to 323 K. The value of ΔS of CO_2 on anthracite is smaller than those of ΔS of CO_2 on 5A and 13X zeolites [33], which indicates that the orderliness of adsorbed CO_2 on 5A and 13X zeolites is higher than that on anthracite.

It is obvious that the entropy loss of CH_4 on anthracite is lower than that of CO_2 at the same condition. Barrer [49] has found that the interaction between permanent quadrupole moment of molecule and electrostatic field can result in a more efficient packing. If the molecule packing is more effective, the larger adsorption heat will be released [33]. Due to the existence of quadrupole moment, the packing manner of CO_2 molecule on anthracite is more efficient, and Q_{st} of CO_2 is greater as shown in Figure 10. Meanwhile, the bigger entropy loss of CO_2 reveals that the adsorbed CO_2 molecules form a more stable configuration, which is also one reason why the sorption amount of CO_2 on coal is larger than that of CH_4. In addition, the entropy losses of both gases decline slightly with the increase of temperature. High temperature will be not conducive to forming a more ordered and stable configuration for adsorbed CH_4 and CO_2, and thus, the sorption quantities of both gases decrease as temperature rises.

4. Conclusions

In this paper, the adsorption isotherms of CH_4 and CO_2 on Qinshui Basin anthracite were obtained at the temperatures of 283 K, 303 K, and 323 K. The adsorption selectivity factor of CO_2 over CH_4 on anthracite was predicted. The affinities and thermodynamic properties of CH_4 and CO_2 on anthracite were investigated. The main conclusions are as follows:

(1) The sorption ability of CO_2 on anthracite is much larger than that of CH_4. At the temperatures of 283 K and 303 K, α_{CO_2/CH_4} quickly increases to the maximum and then slowly declines with the increase of pressure. At 323 K, α_{CO_2/CH_4} monotonously reduces as pressure enhances. CO_2 mole fraction in mixture gases has obvious effect on α_{CO_2/CH_4}. The values of α_{CO_2/CH_4} are more than 4.0, revealing that the technology of CO_2-ECBM is feasible. In actual coal reservoir, low temperature is helpful for injected CO_2 to displace preadsorbed CH_4. Henry's constant of CH_4 is smaller than that of CO_2, and CH_4 has a weaker adsorption affinity with matrix surface

(2) The values of Ω of both gases are more negative with the increase of pressure. The absolute value of Ω of CO_2 is much bigger than that of CH_4, revealing that CO_2 adsorption is more favorable. As pressure increases, the absolute values of ΔG of CO_2 and CH_4 rise. The larger absolute value of ΔG of CO_2 indicates that the degree of spontaneity of CO_2 adsorption is higher

(3) As adsorption loading enhances, Q_{st} of CO_2 increases, while Q_{st} of CH_4 declines. The value of Q_{st} of CO_2 is larger than that of CH_4. With increasing surface coverage, the entropy loss of CH_4 decreases,

while the entropy loss of CO_2 enlarges. Improving temperature will reduce the entropy losses of both gases. The higher entropy loss of CO_2 suggests that the adsorbed CO_2 molecules constitute a more ordered configuration than adsorbed CH_4 molecules

Data Availability

The data used to support the findings of this study are available from the corresponding authors upon request.

Conflicts of Interest

The authors declare that they have no conflicts of interest.

Acknowledgments

This work was supported by the Fund of Key Laboratory for Digital Land and Resources of Jiangxi Province, East China University of Technology (Grant no. DLLJ201914), the Special Youth Project of Science and Technology Innovation Enterprise Capital of China Coal Technology & Engineering Group Co., Ltd. (Grant no. 2018-2-QN016), the Doctoral Startup Foundation of East China University of Technology (Grant no. DHBK2018020), and the Fund of State Key Laboratory of Nuclear Resources and Environment (Grant no. NRE1606).

References

[1] K. Jessen, G. Tang, and A. Kovscek, "Laboratory and simulation investigation of enhanced coalbed methane recovery by gas injection," *Transport in Porous Media*, vol. 73, no. 2, pp. 141–159, 2008.

[2] Z. Liu, Z. Zhang, Y. Lu, S. Choi, and X. Liu, "Sorption hysteresis characterization of CH_4 and CO_2 on anthracite, bituminous coal, and lignite at low pressure," *ASME Journal of Energy Resources Technology*, vol. 140, article 012203, 2018.

[3] M. Mazzotti, R. Pini, and G. Storti, "Enhanced coalbed methane recovery," *The Journal of Supercritical Fluids*, vol. 47, no. 3, pp. 619–627, 2009.

[4] F. Han, A. Busch, B. Kross, Z. Liu, and J. Yang, "CH_4 and CO_2 sorption isotherms and kinetics for different size fractions of two coals," *Fuel*, vol. 108, pp. 137–142, 2013.

[5] J. Zhou, S. Xie, Y. Jiang et al., "Influence of supercritical CO_2 exposure on CH_4 and CO_2 adsorption behaviors of shale: implications for CO_2 sequestration," *Energy & Fuels*, vol. 32, no. 5, pp. 6073–6089, 2018.

[6] X. Du, M. Gu, Z. Liu, Y. Zhao, F. Sun, and T. Wu, "Enhanced shale gas recovery by the injections of CO_2, N_2, and CO_2/N_2 mixture gases," *Energy & Fuels*, vol. 33, no. 6, pp. 5091–5101, 2019.

[7] Z. Wang and X. Tang, "New insights from supercritical methane adsorption in coal: gas resource estimation, thermodynamics, and engineering application," *Energy Fuels*, vol. 32, no. 4, pp. 5001–5009, 2018.

[8] J. Zhang, K. Liu, M. Clennell, D. Dewhurst, and M. Pervukhina, "Molecular simulation of CO_2–CH_4 competitive adsorption and induced coal swelling," *Fuel*, vol. 160, pp. 309–317, 2015.

[9] J. Bae and S. Bhatia, "High-pressure adsorption of methane and carbon dioxide on coal," *Energy & Fuels*, vol. 20, no. 6, pp. 2599–2607, 2006.

[10] A. Busch, Y. Gensterblum, and B. Kross, "Methane and CO_2 sorption and desorption measurements on dry Argonne premium coals: pure components and mixtures," *International Journal of Coal Geology*, vol. 55, no. 2-4, pp. 205–224, 2003.

[11] Y. Song, B. Jiang, and J. Li, "Retracted article: simulations and experimental investigations of the competitive adsorption of CH_4 and CO_2 on low-rank coal vitrinite," *Journal of Molecular Modeling*, vol. 23, no. 10, p. 280, 2017.

[12] H. Yu, R. Jing, P. Wang, L. Chen, and Y. Yang, "Preferential adsorption behaviour of CH_4 and CO_2 on high-rank coal from Qinshui Basin, China," *International Journal of Mining Science and Technology*, vol. 24, no. 4, pp. 491–497, 2014.

[13] J. You, L. Tian, C. Zhang et al., "Adsorption behavior of carbon dioxide and methane in bituminous coal: a molecular simulation study," *Chinese Journal of Chemical Engineering*, vol. 24, no. 9, pp. 1275–1282, 2016.

[14] A. Busch and Y. Gensterblum, "CBM and CO_2-ECBM related sorption processes in coal: a review," *International Journal of Coal Geology*, vol. 87, no. 2, pp. 49–71, 2011.

[15] X. Liu, X. He, N. Qiu et al., "Molecular simulation of CH_4, CO_2, H_2O and N_2 molecules adsorption on heterogeneous surface models of coal," *Applied Surface Science*, vol. 389, pp. 894–905, 2016.

[16] Y. Dang, L. Zhao, X. Lu et al., "Molecular simulation of CO_2/CH_4 adsorption in brown coal: effect of oxygen-, nitrogen-, and sulfur-containing functional groups," *Applied Surface Science*, vol. 423, pp. 33–42, 2017.

[17] W. Zhou, H. Wang, Z. Zhang, H. Chen, and X. Liu, "Molecular simulation of $CO_2/CH_4/H_2O$ competitive adsorption and diffusion in brown coal," *RSC Advance*, vol. 9, no. 6, pp. 3004–3011, 2019.

[18] Z. Liu, *Ad-/Desorption Equilibrium of Coal Reservoir and Its Alterations after Super-Critical CO_2 Exposure*, Chongqing University, Chongqing, China, 2018.

[19] S. Duan, M. Gu, X. Du, and X. Xian, "Adsorption equilibrium of CO_2 and CH_4 and their mixture on Sichuan Basin shale," *Energy & Fuels*, vol. 30, no. 3, pp. 2248–2256, 2016.

[20] X. Song, L. Wang, X. Ma, and Y. Zeng, "Adsorption equilibrium and thermodynamics of CO_2 and CH_4 on carbon molecular sieves," *Applied Surface Science*, vol. 396, pp. 870–878, 2017.

[21] X. Zhou, H. Yi, X. Tang, H. Deng, and H. Liu, "Thermodynamics for the adsorption of SO_2, NO and CO_2 from flue gas on activated carbon fiber," *Chemical Engineering Journal*, vol. 200-202, pp. 399–404, 2012.

[22] M. Mofarahi and A. Bakhtyari, "Experimental investigation and thermodynamic modeling of CH_4/N_2 adsorption on zeolite 13X," *Journal of Chemical and Engineering Data*, vol. 60, no. 3, pp. 683–696, 2015.

[23] L. Zhou, Q. Feng, and Y. Qin, "Thermodynamic analysis of competitive adsorption of CO_2 and CH_4 on coal matrix," *Journal of China Coal Society*, vol. 36, no. 8, pp. 1307–1311, 2011.

[24] K. Dong, F. Zeng, J. Jia, C. Chen, and Z. Gong, "Molecular simulation of the preferential adsorption of CH_4 and CO_2 in middle-rank coal," *Molecular Simulation*, vol. 45, no. 1, pp. 15–25, 2019.

[25] K. Foo and B. Hameed, "Insights into the modeling of adsorption isotherm systems," *Chemical Engineering Journal*, vol. 156, no. 1, pp. 2–10, 2010.

[26] Y. Chen, Z. Qiao, D. Lv et al., "Selective adsorption of light alkanes on a highly robust indium based metal-organic framework," *Industrial Engineering Chemistry Research*, vol. 56, no. 15, pp. 4488–4495, 2017.

[27] A. Myers and J. Prausnitz, "Thermodynamics of mixed-gas adsorption," *AIChE Journal*, vol. 11, no. 1, pp. 121–127, 1965.

[28] R. Shi, D. Lv, Y. Chen et al., "Highly selective adsorption separation of light hydrocarbons with a porphyrinic zirconium metal-organic framework PCN-224," *Separation and Purification Technology*, vol. 207, pp. 262–268, 2018.

[29] W. Liang, H. Xiao, D. Lv, J. Xiao, and Z. Li, "Novel asphalt-based carbon adsorbents with super-high adsorption capacity and excellent selectivity for separation for light hydrocarbons," *Separation and Purification Technology*, vol. 190, pp. 60–67, 2018.

[30] L. Li, X. Wang, J. Liang et al., "Water-stable anionic metal-organic framework for highly selective separation of methane from natural gas and pyrolysis gas," *ACS Applied Materials Interfaces*, vol. 8, no. 15, pp. 9777–9781, 2016.

[31] J. Lu, W. Liu, L. Sun, and X. Liu, "Adsorption equilibrium and separation of methane and carbon dioxide mixtures on 13X molecular sieve," *Journal of Chemical Engineering of Chinese Universities*, vol. 27, no. 1, pp. 1–6, 2013.

[32] W. Liu, L. Sun, and X. Liu, "Adsorption of ethylene and carbon dioxide binary systems on active carbon: experiment and model," *Journal of Chemical Engineering of Chinese Universities*, vol. 26, no. 1, pp. 25–30, 2012.

[33] H. Deng, H. Yi, X. Tang, Q. Yu, P. Ning, and L. Yang, "Adsorption equilibrium for sulfur dioxide, nitric oxide, carbon dioxide, nitrogen on 13X and 5A zeolites," *Chemical Engineering Journal*, vol. 188, pp. 77–85, 2012.

[34] X. Tang, N. Ripepi, N. Stadie, and L. Yu, "Thermodynamic analysis of high pressure methane adsorption in Longmaxi shale," *Fuel*, vol. 193, pp. 411–418, 2017.

[35] A. Myers, "Characterization of nanopores by standard enthalpy and entropy of adsorption of probe molecules," *Colloids and Surfaces A: Physicochemical and Engineering Aspects*, vol. 241, no. 1-3, pp. 9–14, 2004.

[36] F. Ridha and P. Webley, "Entropic effects and isosteric heats of nitrogen and carbon dioxide adsorption on chabazite zeolites," *Microporous and Mesoporous Materials*, vol. 132, no. 1-2, pp. 22–30, 2010.

[37] B. Liu, C. Qi, T. Mai et al., "Competitive adsorption and diffusion of CH_4/CO_2 binary mixture within shale organic nanochannels," *Journal of Natural Gas Science and Engineering*, vol. 53, pp. 329–336, 2018.

[38] J. Fitzgerald, Z. Pan, M. Sudibandriyo Jr., K. G. Robinson, and S. Reeves, "Adsorption of methane, nitrogen, carbon dioxide and their mixtures on wet Tiffany coal," *Fuel*, vol. 84, no. 18, pp. 2351–2363, 2005.

[39] F. Liu, K. Ellett, Y. Xiao, and J. Rupp, "Assessing the feasibility of CO_2 storage in the New Albany Shale (Devonian-Mississippian) with potential enhanced gas recovery using reservoir simulation," *International Journal of Greenhouse Gas Control*, vol. 17, pp. 111–126, 2013.

[40] Y. He, X. Fu, and L. Lu, "Differences of H_2S, CH_4 and N_2 adsorption ability on coal," *China Sciencepaper*, vol. 11, no. 15, pp. 1775–1777, 2016.

[41] X. Tang, N. Ripepi, N. Stadie, L. Yu, and M. Hall, "A dual-site Langmuir equation for accurate estimation of high pressure deep shale gas resources," *Fuel*, vol. 185, pp. 10–17, 2016.

[42] L. Brochard, M. Vandamme, R. Pellenq, and T. Chong, "Adsorption-induced deformation of microporous materials: coal swelling induced by CO_2-CH_4 competitive adsorption," *Langmuir*, vol. 28, no. 5, pp. 2659–2670, 2012.

[43] S. Duan, *A Thermodynamics Study of CO_2 and CH_4 Adsorption on Sichuan Basin Shales*, Chongqing University, Chongqing, China, 2017.

[44] S. Bhadra, A. Ebner, and J. Ritter, "On the use of the dual process Langmuir model for predicting unary and binary isosteric heats of adsorption," *Langmuir*, vol. 28, no. 17, pp. 6935–6941, 2012.

[45] A. Chakraborty, B. Saha, and S. Koyama, "On the thermodynamic modeling of the isosteric heat of adsorption and comparison with experiments," *Applied Physics Letters*, vol. 89, article 171901, 2006.

[46] T. Hill, "Statistical mechanics of adsorption. V. Thermodynamics and heat of adsorption," *The Journal of Chemical Physics*, vol. 17, no. 6, pp. 520–535, 1949.

[47] Z. He, G. Yu, and D. Barba, "Effect of molecular dimension and shape on hindered diffusion of macromolecules in micropores," *Journal of Chemical Industry and Engineering (China)*, vol. 44, no. 2, pp. 143–150, 1993.

[48] T. Zhang, G. Ellis, S. Ruppel, K. Milliken, and R. Yang, "Effect of organic-matter type and thermal maturity on methane adsorption in shale-gas systems," *Organic Geochemistry*, vol. 47, pp. 120–131, 2012.

[49] R. Barrer, *Zeolite and Clay Minerals*, Academic Press, New York, NY, USA, 1978.